

LETTERS

Evidence for wavelike energy transfer through quantum coherence in photosynthetic systems

Gregory S. Engel^{1,2}, Tessa R. Calhoun^{1,2}, Elizabeth L. Read^{1,2}, Tae-Kyu Ahn^{1,2}, Tomáš Mančal^{1,2,†}, Yuan-Chung Cheng^{1,2}, Robert E. Blankenship^{3,4} & Graham R. Fleming^{1,2}

Photosynthetic complexes are exquisitely tuned to capture solar light efficiently, and then transmit the excitation energy to reaction centres, where long term energy storage is initiated. The energy transfer mechanism is often described by semiclassical models that invoke ‘hopping’ of excited-state populations along discrete energy levels^{1,2}. Two-dimensional Fourier transform electronic spectroscopy^{3–5} has mapped⁶ these energy levels and their coupling in the Fenna–Matthews–Olson (FMO) bacteriochlorophyll complex, which is found in green sulphur bacteria and acts as an energy ‘wire’ connecting a large peripheral light-harvesting antenna, the chlorosome, to the reaction centre^{7–9}. The spectroscopic data clearly document the dependence of the dominant energy transport pathways on the spatial properties of the excited-state wavefunctions of the whole bacteriochlorophyll complex^{6,10}. But the intricate dynamics of quantum coherence, which has no classical analogue, was largely neglected in the analyses—even though electronic energy transfer involving oscillatory populations of donors and acceptors was first discussed more than 70 years ago¹¹, and electronic quantum beats arising from quantum coherence in photosynthetic complexes have been predicted^{12,13} and indirectly observed¹⁴. Here we extend previous two-dimensional electronic spectroscopy investigations of the FMO bacteriochlorophyll complex, and obtain direct evidence for remarkably long-lived electronic quantum coherence playing an important part in energy transfer processes within this system. The quantum coherence manifests itself in characteristic, directly observable quantum beating signals among the excitons within the *Chlorobium tepidum* FMO complex at 77 K. This wavelike characteristic of the energy transfer within the photosynthetic complex can explain its extreme efficiency, in that it allows the complexes to sample vast areas of phase space to find the most efficient path.

In two-dimensional Fourier transform electronic spectroscopy, three pulses and a strongly attenuated local oscillator are incident on the sample. (For a detailed description of the method and the apparatus used in this study, see refs 3, 5, 15.) In the simplest time domain representation, the first pulse creates a coherence that evolves for time τ , then the second pulse creates an excited-state population that evolves for time T , and the third pulse creates a coherence that accumulates phase in the opposite direction for time t before rephasing occurs and a signal pulse is emitted in the unique phase-matched direction. The full electric field of the signal pulse is measured through heterodyne detection using spectral interferometry. In a frequency domain representation, two-dimensional Fourier transform electronic spectroscopy probes electronic couplings and energy transfer in molecules by mapping how excitations before the population time T affect emission after the population

time. The coherence wavelength represents the initial excitation, while the rephasing wavelength can be thought of as the subsequent emission. Without coupling, contributions from excited-state absorption and emission cancel each other, yielding no off-diagonal peaks in the spectrum that signal such coupling. But in the presence of coupling, the cancellation is no longer complete and a so-called cross-peak emerges¹⁶. Two-dimensional spectroscopy thus provides an excellent probe of the coupling between energy levels.

In the present experiment, we use two-dimensional electronic spectroscopy to observe oscillations caused by electronic coherence evolving during the population time in FMO. Such quantum coherence, a coherent superposition of electronic states analogous to a nuclear wavepacket in the vibrational regime, is formed when the system is initially excited by a short light pulse with a spectrum that spans multiple exciton transitions. Theoretical predictions indicate that both the amplitudes and shapes of peaks will contain beating signals with frequencies corresponding to the differences in energy between component exciton states¹⁷.

To observe the quantum beats, two-dimensional spectra were taken at 33 population times T , ranging from 0 to 660 fs. Representative spectra are shown in Fig. 1 and a video of the spectral evolution is included in the Supplementary Information. In these spectra, the lowest-energy exciton gives rise to a diagonal peak near 825 nm that clearly oscillates: its amplitude grows, fades, and subsequently grows again. The peak’s shape evolves with these oscillations, becoming more elongated when weaker and rounder when the signal amplitude intensifies. The associated cross-peak amplitude also appears to oscillate. Surprisingly, the quantum beating lasts for 660 fs. This observation contrasts with the general assumption that the coherences responsible for such oscillations are destroyed very rapidly, and that population relaxation proceeds with complete destruction of coherence² (so that the transfer of electronic coherence between excitons during relaxation is usually ignored^{2,18,19}).

We note that this issue has been discussed theoretically, and that some theoretical models include coherence among both donors and acceptors²⁰; however, coherence must be treated between all chromophores to ensure that the model will accurately reproduce the dynamics of the system²¹. In the case of FMO, theoretical models indicate that electronic coherence should dephase on the timescale of the initial population transfer, established by experiment to be less than 250 fs for all but excitons 1 and 3 (refs 2, 22). The strong quantum beating that we observe to last for at least 660 fs clearly exceeds the model predictions. We believe that to account for this long-lived coherence and provide an accurate description of the system, the protein must have a more active role in a realistic bath model; that is, it must be allowed to interact with both donors and

¹Department of Chemistry & QB3 Institute, University of California, Berkeley, ²Physical Biosciences Division, Lawrence Berkeley National Laboratory, Berkeley, California 94720, USA. ³Department of Biology, ⁴Department of Chemistry, Washington University, St Louis, Missouri 63130, USA. †Present address: Institute of Physics of Charles University, 12116 Prague 2, Czech Republic.

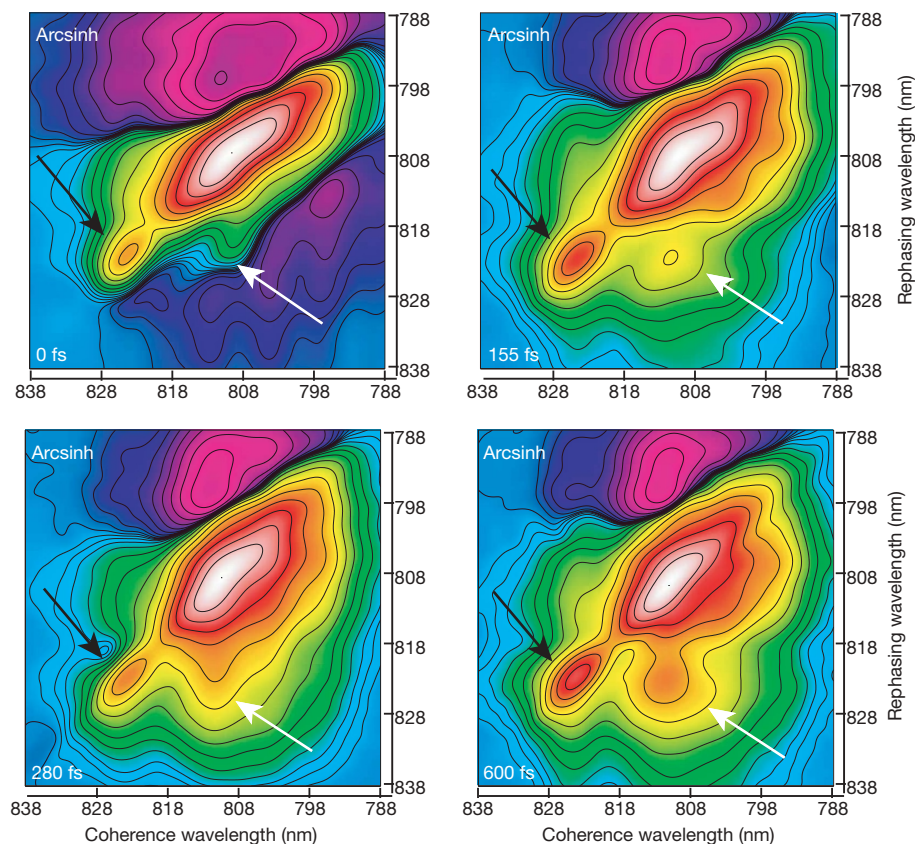


Figure 1 | Two-dimensional electronic spectra of FMO. Selected two-dimensional electronic spectra of FMO are shown at population times from $T = 0$ to 600 fs demonstrating the emergence of the exciton 1–3 cross-peak (white arrows), amplitude oscillation of the exciton 1 diagonal peak (black arrows), the change in lowest-energy exciton peak shape and the oscillation of the 1–3 cross-peak amplitude. The data are shown with an arcsinh coloration to highlight smaller features: amplitude increases from blue to white (for a three-dimensional representation of the coloration see Fig. 3a).

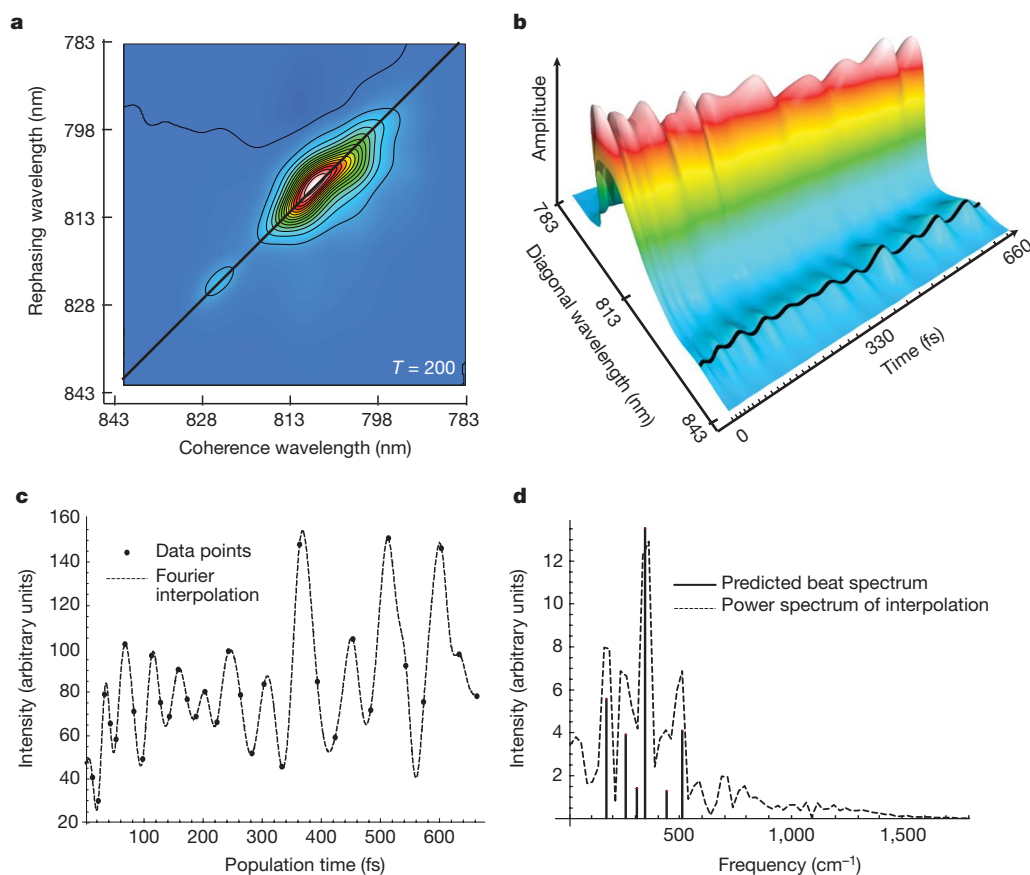


Figure 2 | Electronic coherence beating. **a**, A representative two-dimensional electronic spectrum with a line across the main diagonal peak. The amplitude along this diagonal line is plotted against population time in **b** with a black line covering the exciton 1 peak amplitude; the data are scaled by a smooth function effectively normalizing the data without affecting oscillations. A spline interpolation is used to connect the spectra; the times at which spectra were taken are denoted by tick marks along the time axis. **c**, The amplitude of the peak corresponding to exciton 1 shown with a dotted Fourier interpolation. **d**, The power spectrum of the Fourier interpolation in **c** is plotted with the theoretical spectrum showing beats between exciton 1 and excitons 2–7.

acceptors, to enable coherence transfer and possibly the generation of new coherences.

Our further investigation of these spectral oscillations focuses on the best-resolved spectral features in the two-dimensional electronic spectra, that is, the lowest exciton diagonal peak and associated cross-peak. In Fig. 2, we show the amplitude oscillations with time along the main diagonal of the spectrum. Because of the non-uniform spacing of the data points, converting the data to a unique power spectrum is not possible; instead, we map the data onto a Fourier subspace using a non-uniform fast Fourier transform algorithm²³. The sampled amplitude variations of the lowest-energy exciton are shown with a Fourier interpolation from the subspace that was selected to be maximally consistent with the excitonic model. The theoretical excitonic coherence line spectrum was calculated using the exciton energies from the hamiltonian in ref. 6, and the relative amplitudes were calculated using orientationally averaged response magnitudes for the associated cross-peak pathways^{16,24,25}.

The agreement between the data, the Fourier interpolation and the theoretical exciton spectrum demonstrates that the quantum beating observed is fully consistent with electronic coherence (analyses of beating in more peaks are shown in the Supplementary Information), and we present comparisons to an independent theoretical lineshape prediction to confirm this conclusion. Further, because the predicted orientational factor is identical for a diagonal exciton beating and for a cross-peak, that the amplitude of the beat is of the order of the amplitude of the cross-peak even at long times (>500 fs) indicates that the electronic coherence can play a significant role in determining the overall relaxation dynamics within the protein complex. This observation suggests that coherence relaxation pathways, including coherence transfer, should no longer be disregarded in theoretical models of photosynthetic protein complexes.

A predicted¹⁷ signature of quantum beating in a dimer system is out-of-phase modulation of the diagonal and anti-diagonal widths of a peak relative to its amplitude, with the peak predicted to become rounder as it gets stronger. Figure 3 documents precisely this behaviour in the lowest exciton state. We note that if this oscillation were due to vibrational wavepacket motion, the exciton peak would be expected instead to oscillate in frequency but maintain constant volume. The peak shape oscillations we see have not previously been observed in two-dimensional spectra, in which the peak width along the anti-diagonal direction is generally an indicator of the extent of homogeneous broadening, whereas the peak width along the diagonal provides a measure of inhomogeneous broadening. In this context, the width modulation we observe would be akin to losing memory of the initial state, and subsequently regaining that memory. Clearly, this interpretation is not applicable while coherence persists. The unusual nature of the width modulation evident in our data and its agreement with the predicted¹⁷ characteristics of quantum beating further strengthens our conclusion that the beating we measure is due to excitonic quantum coherence.

Figure 4 shows that a Fourier interpolation of the beating spectrum apparent in the cross-peak between excitons 1 and 3 can again be explained by the expected exciton beating spectrum. The beating signal shows frequency components from all excitons coupled to either excitons 1 or 3, and a very strong component from the beat frequency between the two coupled excitons (1 and 3) that give rise to the cross peak. However, the cross-peak amplitude and associated beating do not appear strongly at time $T = 0$; this provides strong evidence for the existence of electronic coherence transfer in this system, with one superposition, for example between excitons 3 and 5, transferred into a superposition between excitons 3 and 1.

The observations illustrated in Figs 2–4 clearly demonstrate that any full description of FMO dynamics needs to account for coherence between donors and acceptors, and for coherence transfer on a similar timescale to population relaxation. While our spectra are recorded at 77 K and the coherence among members of the ensemble

will dephase faster at higher temperatures, quantum coherence will also be important at higher temperatures. This is because the underlying hamiltonian, dynamics and relaxation pathways associated with superposition states of individual complexes do not depend on dephasing of the ensemble properties observed in a measurement. In an ensemble sense, the presence of quantum coherence means that the mean square displacement of the initial excitation from a quantum walk increases quadratically with time rather than linearly as in diffusive hopping of excitation²⁶.

But a more microscopic picture of the implications of such quantum coherence for energy transfer can be found by considering an individual complex: superposition states formed during a fast excitation event allow the excitation to reversibly sample relaxation rates from all component exciton states, thereby efficiently directing the energy transfer to find the most effective sink for the excitation energy (which, in the isolated FMO complex, is the lowest energy state). When viewed in this way, the system is essentially performing a single quantum computation, sensing many states simultaneously and selecting the correct answer, as indicated by the efficiency of the energy transfer. In the presence of quantum coherence transfer, such an operation is analogous to Grover's algorithm, with the hamiltonian describing both relaxation to the lowest energy state and coherence transfer (refilling the coherence lost from the transfer to the lowest-energy state)²⁷; such a scheme can provide efficiency beyond

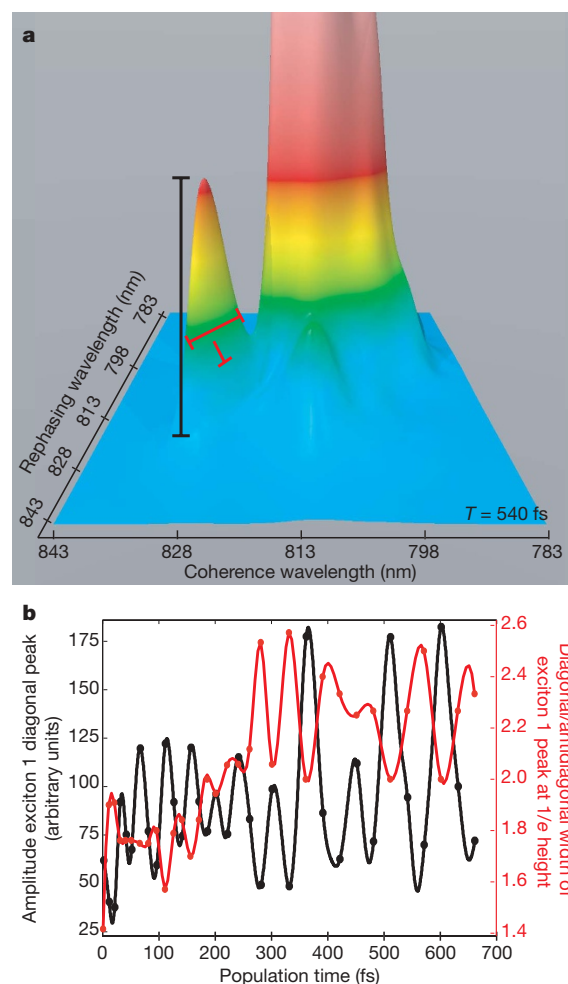


Figure 3 | Characteristic anticorrelation between peak amplitude and width. The anticorrelation shown in **b** between the amplitude of the diagonal exciton peak (black line in **a**) and the ratio of the diagonal to anti-diagonal widths of the peak (red lines in **a**) is a characteristic predicted from theory for exciton quantum beating¹⁷. This pattern would not arise from phonon coupling and highlights the change in integrated line strength associated with quantum beating.

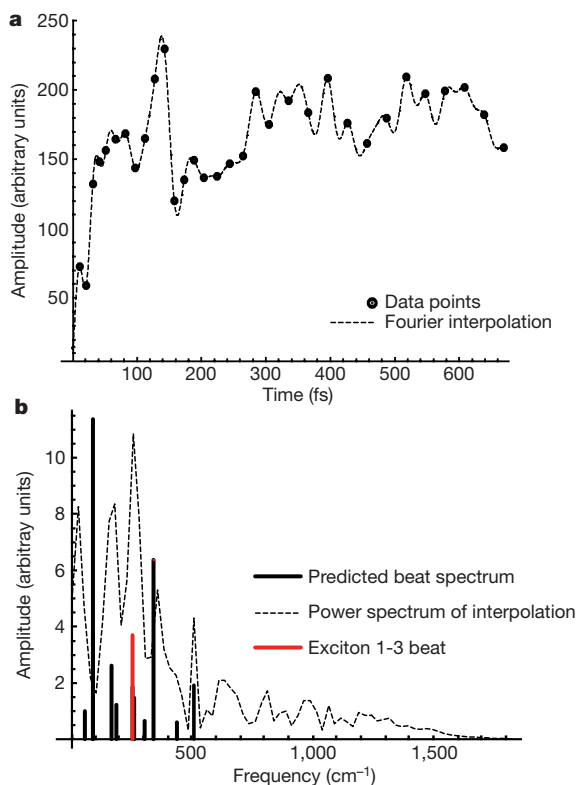


Figure 4 | Quantum beating in cross peaks. **a**, The raw amplitude of the exciton 1–3 cross-peak, with a Fourier interpolation of the points (dotted line). **b**, The power spectrum of this interpolation (dotted line), the exciton beating line spectra of both excitons 1 and 3 (black), and the 1–3 beat frequency (red). We expect that the other frequencies may couple to this cross-peak but that the dominant frequency corresponds to the red transition. The apparent low-frequency peak is due to the growth of the cross-peak amplitude and appears as a peak because the data were de-meaned (mean subtracted from the data) before the transform to improve numerical accuracy, pinning the zero-frequency component to zero.

that of a classical search algorithm. This mechanism contrasts with a semiclassical ‘hopping’ mechanism through which the excitation moves stepwise from exciton state to exciton state, dissipating energy at each step, which would be similar to a classical search where only one state can be occupied at any one time. Such a mechanism also raises the possibility of non-local events, although more detailed analysis is needed before we can determine whether such effects are present in FMO.

The FMO light-harvesting complex provides an opportunity to apply more complete energy transfer theories that invoke non-markovian dynamics and include coherence transfer. Such theories need to include wavelike energy motion owing to long-lived coherence terms, alongside the population transfer included in current models. Further, the observed preservation of coherence in this photosynthetic system requires us to redefine our description of the role of electron–phonon interactions within photosynthetic proteins. In particular, the protein may not only enforce the structure that gives rise to the couplings, but also modulate those couplings with motions of charged residues and changing local dielectric environments, which will change exciton energies and promote coherence transfer.

METHODS

Sample preparation. The FMO sample was isolated from *Chlorobium tepidum* as published previously⁹. The sample was dissolved in a buffer of 800 mM tris/HCl pH 8.0, 50 mM NaCl with 0.1% lauryldimethylamine oxide as a detergent. The sample was then mixed 65:35 v/v in glycerol, placed in a 200 μ m quartz cell (Starna). The sample was cooled in a cryostat (Oxford Instruments) to 77 K. The absorbance of the sample at 805 nm was then measured to be 0.16.

Data acquisition. A home-built oscillator was used to seed a home-built regenerative amplifier to produce a 3.4 kHz pulse train of 41 fs pulses centred about 808 nm with a spectral width of 31 nm full-width at half-maximum (FWHM)²⁸. The stability of the laser system through the data acquisition period was measured to be 0.28% to 0.44%. The laser pulse width was measured with both autocorrelation (38 fs FWHM) and frequency resolved optical gating (FROG) (41 fs FWHM).

A diffractive optic was used to create two pairs of phase-locked beams, and all beams were incident on the same optics, aside from the one-degree fused silica wedges (Almaz Optics) used for delay stages. The delay stages were calibrated using spectral interferometry and have been shown to have attosecond stability and reproducibility^{3,29}. During data collection, the coherence time was stepped in 4 fs steps from –600 to 600 fs. Population times were sampled at 0, 10, 20, 30, 40, 50, 65, 80, 95, 110, 125, 140, 155, 170, 185, 200, 220, 240, 260, 280, 300, 330, 360, 390, 420, 450, 480, 510, 540, 570, 600, 630 and 660 fs. Additional points were taken at –1,000 fs to ensure that the signal observed was not an artefact. The sample was moved after every third data point, and some data points were repeated to ensure that the sample was not degrading during measurements.

The local oscillator was attenuated with a neutral density filter combination of absorbance 3.5 at 800 nm. The total power incident on the sample was 15 nJ (5 nJ per pulse) focused to a spot size of less than 70 μ m. The resulting signal and heterodyne beam were frequency-resolved with a spectrometer (Acton Research) and captured on a 1,340 \times 5 pixel region of our charge-coupled device (CCD) array (Princeton Instruments). Scatter subtraction, Fourier windowing and transformation to frequency–frequency space was done as reported previously^{3,15}. Pump–probe data were taken for accurate phasing of the two dimensional spectra.

Data modelling. To model the beat patterns in the data series, a non-uniform fast Fourier transform algorithm was used to search for Fourier power series that matched the data and were consistent with expected power spectrum. Because of the unequal spacing, a unique answer does not exist. The non-uniform fast Fourier transform power spectra were estimated using a modified 4th-Jackson kernel, and the results were then transformed back using a standard fast Fourier transform library (FFTW; www.fftw.org)^{23,30}. To scale the data and eliminate spectral components from population dynamics, a smooth function with an exponential growth of the order of the pulse width and an exponential decay matched to the population dynamics in the main peak was used.

Received 13 October 2006; accepted 14 February 2007.

- Blankenship, R. E. *Molecular Mechanisms of Photosynthesis* (Blackwell Science, Oxford/Malden, 2002).
- van Amerongen, H., Valkunas, L. & van Grondelle, R. *Photosynthetic Excitons* (World Scientific, Singapore/River Edge, 2000).
- Brixner, T., Mančal, T., Stiopkin, I. V. & Fleming, G. R. Phase-stabilized two-dimensional electronic spectroscopy. *J. Chem. Phys.* **121**, 4221–4236 (2004).
- Jonas, D. M. Two-dimensional femtosecond spectroscopy. *Annu. Rev. Phys. Chem.* **54**, 425–463 (2003).
- Cowan, M. L., Ogilvie, J. P. & Miller, R. J. D. Two-dimensional spectroscopy using diffractive optics based phased-locked photon echoes. *Chem. Phys. Lett.* **386**, 184–189 (2004).
- Brixner, T. et al. Two-dimensional spectroscopy of electronic couplings in photosynthesis. *Nature* **434**, 625–628 (2005).
- Fenna, R. E. & Matthews, B. W. Chlorophyll arrangement in a bacteriochlorophyll protein from *Chlorobium limicola*. *Nature* **258**, 573–577 (1975).
- Li, Y. F., Zhou, W. L., Blankenship, R. E. & Allen, J. P. Crystal structure of the bacteriochlorophyll a protein from *Chlorobium tepidum*. *J. Mol. Biol.* **271**, 456–471 (1997).
- Camara-Artigas, A., Blankenship, R. E. & Allen, J. P. The structure of the FMO protein from *Chlorobium tepidum* at 2.2 angstrom resolution. *Photosynth. Res.* **75**, 49–55 (2003).
- Cho, M. H. et al. Exciton analysis in 2D electronic spectroscopy. *J. Phys. Chem. B* **109**, 10542–10556 (2005).
- Perrin, F. Théorie quantique des transferts d’activation entre molécules de même espèce. Cas des solutions fluorescentes. *Ann. Phys. (Paris)* **17**, 283–314 (1932).
- Knox, R. S. Electronic excitation transfer in the photosynthetic unit: Reflections on work of William Arnold. *Photosynth. Res.* **48**, 35–39 (1996).
- Leegwater, J. A. Coherent versus incoherent energy transfer and trapping in photosynthetic antenna complexes. *J. Phys. Chem.* **100**, 14403–14409 (1996).
- Savikhin, S., Buck, D. R. & Struve, W. S. Oscillating anisotropies in a bacteriochlorophyll protein: Evidence for quantum beating between exciton levels. *Chem. Phys.* **223**, 303–312 (1997).
- Brixner, T., Stiopkin, I. V. & Fleming, G. R. Tunable two-dimensional femtosecond spectroscopy. *Opt. Lett.* **29**, 884–886 (2004).
- Cho, M. H. & Fleming, G. R. The integrated photon echo and solvation dynamics. II. Peak shifts and two-dimensional photon echo of a coupled chromophore system. *J. Chem. Phys.* **123**, 114506 (2005).
- Pisliakov, A. V., Mančal, T. & Fleming, G. R. Two-dimensional optical three-pulse photon echo spectroscopy. II. Signatures of coherent electronic motion and

- exciton population transfer in dimer two-dimensional spectra. *J. Chem. Phys.* **124**, 234505 (2006).
18. Abramavicius, D., Valkunas, L. & van Grondelle, R. Exciton dynamics in ring-like photosynthetic light-harvesting complexes: A hopping model. *Phys. Chem. Chem. Phys.* **6**, 3097–3105 (2004).
 19. Renger, T., May, V. & Kuhn, O. Ultrafast excitation energy transfer dynamics in photosynthetic pigment-protein complexes. *Phys. Rep. Rev. Phys. Lett.* **343**, 138–254 (2001).
 20. Jang, S. J., Newton, M. D. & Silbey, R. J. Multichromophoric Forster resonance energy transfer. *Phys. Rev. Lett.* **92**, 9312–9323 (2004).
 21. Novoderezhkin, V., Wendling, M. & van Grondelle, R. Intra- and interband transfers in the b800-b850 antenna of *Rhodospirillum rubrum*: Redfield theory modeling of polarized pump-probe kinetics. *J. Phys. Chem. B* **107**, 11534–11548 (2003).
 22. Vulto, S. I. E. *et al.* Excited state dynamics in FMO antenna complexes from photosynthetic green sulfur bacteria: A kinetic model. *J. Phys. Chem. B* **103**, 8153–8161 (1999).
 23. Potts, D. & Kunis, S. Stability results for scattered data interpolation by trigonometric polynomials. (<http://arxiv.org/pdf/math.NA/0702019>) (2007).
 24. Dreyer, J., Moran, A. M. & Mukamel, S. Tensor components in three pulse vibrational echoes of a rigid dipeptide. *Bull. Korean Chem. Soc.* **24**, 1091–1096 (2003).
 25. Hochstrasser, R. M. Two-dimensional IR-spectroscopy: polarization anisotropy effects. *Chem. Phys.* **266**, 273–284 (2001).
 26. Kempe, J. Quantum random walks: An introductory overview. *Contemp. Phys.* **44**, 307–327 (2003).
 27. Grover, L. K. Quantum mechanics helps in searching for a needle in a haystack. *Phys. Rev. Lett.* **79**, 325–328 (1997).
 28. Joo, T., Jia, Y. W. & Fleming, G. R. Ti-sapphire regenerative amplifier for ultrashort high-power multikilohertz pulses without an external stretcher. *Opt. Lett.* **20**, 389–391 (1995).
 29. Lepetit, L., Cheriaux, G. & Joffe, M. Linear techniques of phase measurement by femtosecond spectral interferometry for applications in spectroscopy. *J. Opt. Soc. Am. B* **12**, 2467–2474 (1995).
 30. Frigo, M. & Johnson, S. G. The design and implementation of fftw3. *Proc. IEEE* **93**, 216–231 (2005).

Supplementary Information is linked to the online version of the paper at www.nature.com/nature.

Acknowledgements We thank D. Zigmantas for discussions and J. Wen for purification of the sample. This work was supported by the DOE (at LBNL, UC Berkeley and Washington Univ.). G.S.E. thanks the Miller Institute for Basic Research in Science for support. T.-K.A. was supported by the Korea Research Foundation Grant funded by the Korean government (MOEHRD).

Author Contributions G.S.E., T.R.C., T.-K.A. and E.L.R. prepared the cryogenic sample and collected the data; G.S.E., E.L.R., T.M. and Y.-C.C. performed the data analysis. R.E.B. grew, isolated and purified the FMO sample. G.S.E. wrote the paper, and all authors discussed the results and commented on the manuscript. G.R.F. provided guidance throughout the experiment and analysis and helped to write the manuscript.

Author Information Reprints and permissions information is available at www.nature.com/reprints. The authors declare no competing financial interests. Correspondence and requests for materials should be addressed to G.R.F. (grfleming@lbl.gov).